



New 5D Hyperchaotic System Derived from the Sprott C System: Properties and Anti Synchronization

Saad Fawzi Al-Azzawi*^{ORCID}, Anmar M. Hasan^{ORCID}

Department of Mathematics, College of Computer Science and Mathematics, University of Mosul, 41002 Mosul, Iraq

* Correspondence: Saad Fawzi Al-Azzawi (saad.alazawi@uomosul.edu.iq)

Received: 05-08-2023

Revised: 06-18-2023

Accepted: 06-23-2023

Citation: S. F. Al-Azzawi, and A. M. Hasan, “New 5D hyperchaotic system derived from the Sprott C system: Properties and anti synchronization,” *J. Intell Syst. Control*, vol. 2, no. 2, pp. 110–122, 2023. <https://doi.org/10.56578/jisc020205>.



© 2023 by the author(s). Published by Acadlore Publishing Services Limited, Hong Kong. This article is available for free download and can be reused and cited, provided that the original published version is credited, under the CC BY 4.0 license.

Abstract: This study introduces a new ten-term 5-D hyperchaotic system, derived from the 3-D Sprott C system. The proposed system has coexisting two attractors: the self-excited and hidden attractors. This system exhibits a rich array of characteristics, taking inspiration from various forms of equilibrium points, stable focus-nodes, saddle-focus, and non-hyperbolic unstable points. These features are shown to be dependent on parameter adjustments. The coexistence of chaotic and hyperchaotic attractors within a 5-D system coupled with three types of equilibrium points is an intriguing phenomenon. A spectrum of numerical methodologies, including phase portraits, computation of Lyapunov exponent, estimation of Lyapunov dimension, and multistability analysis, have been employed to effectively illustrate the diverse attractors. The stability theory is utilized for investigating the synchronization problem, a topic that is elucidated in depth. An assortment of dynamical behavior, such as hyperchaotic, hyperchaotic with 2-tours, chaotic, and chaotic with 2-tours, is recognized. Validation of the primary findings is conducted via theoretical and numerical simulations, fortifying the theoretical conclusions, with numerical simulations executed using MATLAB2021.

Keywords: Novel 5D system; Hidden attractors; Coupling and feedback strategy; Non-hyperbolic; Anti-synchronization

1 Introduction

Chaotic and hyperchaotic systems have garnered significant attention from the scientific community in the recent past, due to their promising applicability in diverse areas, including but not limited to, cryptosystems, data encryption [1–4], neural networks [5], synchronization [6], robotics [7], and electronic circuits [8]. The concept of a hidden attractor was first unveiled by Kuznetsov et al. in 2010, but it remained relatively unnoticed until the development of Chua’s circuit by Leonov et al. [9] in 2011. Consequently, systems are now generally classified as possessing either self-excited or hidden attractors. Notably, renowned classical 3-D systems such as the Lorenz system [10], Rossler’s system [11], and most Sprott systems (with the exception of the Sprott A system) [12], harbor self-excited attractors.

Hidden attractors in dynamical systems can be categorized into three types [13–24], whereas self-excited attractors conform to one type [25–30], as depicted in Figure 1. However, the existence of systems incorporating both self-excited and hidden attractors has largely been overlooked in prior research [31]. This gap in knowledge prompted the unveiling of a unique, relatively simple 5-D system showcasing coexistence of multiple attractors and a spectrum of behaviors. A tabulated summary of various 5-D systems with self-excited and hidden attractors is presented in Table 1. This study contributes to the field by introducing:

- A novel 5-D hyperchaotic system, derived from the 3-D Sprott C system.
- This system harbors two fundamental types of multi-attractors (self-excited and hidden).
- The presence of two equilibria points, stable and unstable, lends to a variety of attractors.
- Simplicity is showcased in this system through its composition of merely ten terms, as exhibited in Table 1.
- It bears three positive Lyapunov exponents and possesses a higher Largest Kaplan-York Dimension in comparison to ten other systems, as elucidated in Table 1.
- The system comprises three types of equilibria points: focus-nodes, saddle-focus, and non-hyperbolic.
- Implementation of anti-synchronization is demonstrated.

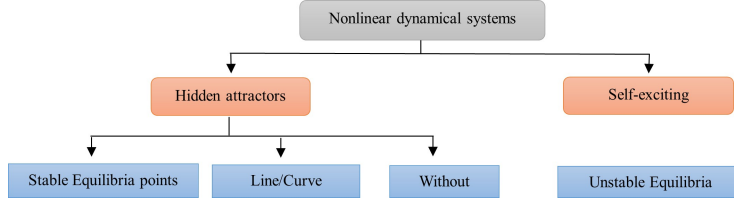


Figure 1. Classification of the attractors of nonlinear dynamical systems

Table 1. Summary of various types of 5-dimensional dynamic systems

No.	System Behavior	No. +ve LE_s	No. Term	Lyapunov Dimension D_L	Attractors Behavior	References
1	Hyperchaotic	n-3	17	3.9785	Self-excited	2018 [32]
2	Hyperchaotic	n-3	17	3.0011	Hidden	2019 [18]
3	Hyperchaotic	n-2	15	4.0502	Hidden	2015 [33]
4	Chaotic	n-4	13	-	Hidden	2020 [16]
5	Hyperchaotic	n-3	13	4.0216	Hidden	2018 [34]
6	Hyperchaotic	n-3	13	4.0216	Hidden	2019 [35]
7	Hyperchaotic	n-2	12	4.0669	Self-excited	2009 [36]
8	Hyperchaotic	n-3	11	3.1899	Hidden	2021 [37]
9	Chaotic	n-4	9	4.002	Hidden	2022 [38]
10	Hyperchaotic	n-2	13	4.189	Self-excited	2022 [39]
11	Hyperchaotic	n-2	10	4.3801	Multi-Attractors (Hidden & Self-excited)	This work

2 Derivation of the Novel 5D Hyperchaotic System

In his seminal work in 1994, Sprott presented nineteen simple chaotic systems, inclusive of the Sprott C system, which can be represented as follows [12]:

$$\begin{cases} \dot{x}_1 = x_2 x_3 \\ \dot{x}_2 = x_1 - x_2 \\ \dot{x}_3 = 1 - x_1^2 \end{cases} \quad (1)$$

where, x_1, x_2 , and x_3 are variables of the system. This system presents two equilibria points $E_{1,2}(\pm 1, \pm 1, 0)$. With Lyapunov exponents of the chaotic system $LE_i = (0.163, 0, -1.163)$, and the corresponding Lyapunov dimension ($D_L = 2.140$). The roots $\lambda_1 = -1, \lambda_2 = \mp 1.4142i$, therefore, classify the system's equilibrium points as non-hyperbolic and unstable.

Expanding upon system (1) and leveraging the principles of the state feedback control [39, 40] and coupling strategy [40–42], a new 5D hyperchaotic system was devised, expressed as follows:

$$\begin{cases} \dot{x}_1 = x_2 x_3 - c x_5 \\ \dot{x}_2 = x_1 - x_2 \\ \dot{x}_3 = 1 - x_1^2 \\ \dot{x}_4 = a x_1 x_3 + b x_4 \\ \dot{x}_5 = x_1 + p x_2 x_3 \end{cases} \quad (2)$$

This system (2) encompasses ten terms, with x_1, x_2, x_3, x_4, x_5 as variables, a, b , and c, p are coupling and control parameters, respectively ($c, b \neq 0$). It can be observed in Figure 2 that the 5-D system (2) demonstrates hyperchaotic behavior when parameters and initial conditions (ICs) from Eq. (3) and Eq. (4) are applied:

$$\begin{cases} a = 1 \\ b = 0.3 \\ c = 0.006 \\ p = 1 \end{cases} \quad (3)$$

$$X(0) = (0.1, 0.1, 0.2, 0.1, 0.2) \quad (4)$$

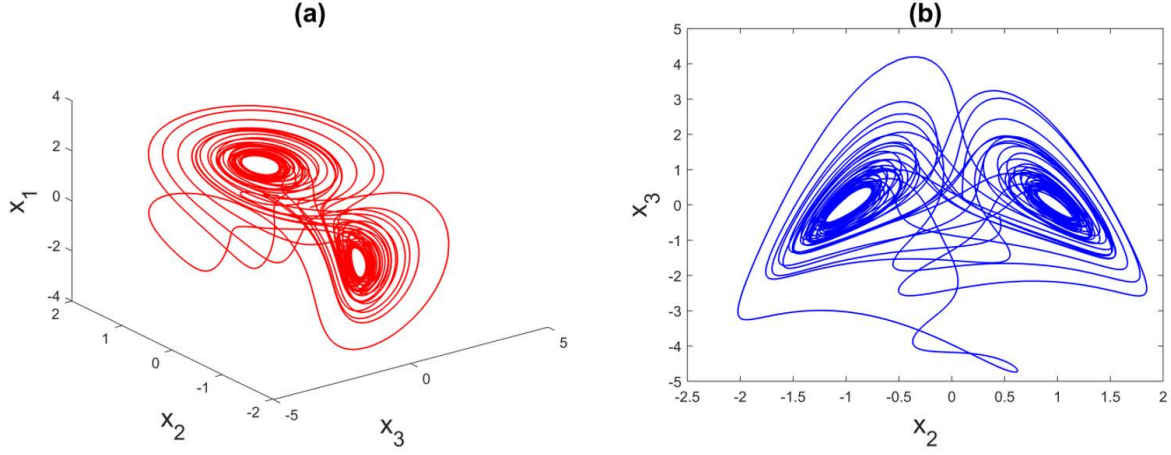


Figure 2. Phase portrait illustrating the behavior of the system (2)

3 Dynamic Properties of New System

The dynamic characteristics of the newly proposed system, System (2), were investigated. By solving the following equations, derived from System (2):

$$\begin{cases} x_2x_3 - cx_5 = 0 \\ x_1 - x_2 = 0 \\ 1 - x_1^2 = 0 \\ ax_1x_3 + bx_4 = 0 \\ x_1 + px_2x_3 = 0 \end{cases} \quad (5)$$

Two equilibrium points, denoted $E_{1,2}$, were determined to be

$$E_{1,2} \left(\pm 1, \pm 1, -\frac{1}{p}, \pm \frac{a}{bp}, \mp \frac{1}{cp} \right) \quad (6)$$

System (2)'s Jacobian matrix at point E_1 is given by

$$J(E_1) = \begin{bmatrix} 0 & -1/p & 1 & 0 & -c \\ 1 & -1 & 0 & 0 & 0 \\ -2 & 0 & 0 & 0 & 0 \\ -a/p & 0 & a & b & 0 \\ 1 & -1 & p & 0 & 0 \end{bmatrix} \quad (7)$$

The corresponding characteristic equation via the law $|J - \lambda I| = 0$ is

$$\lambda^5 + \underbrace{(1-b)}_{A_1} \lambda^4 + \underbrace{\left(2-b+c+\frac{1}{p}\right)}_{A_2} \lambda^3 + \underbrace{\left(2-2b-bc-2cp-\frac{b}{p}\right)}_{A_3} \lambda^2 + \underbrace{(2bcp-2b-2cp)}_{A_4} \lambda + \underbrace{2bcp}_{A_5} = 0 \quad (8)$$

System (2) can be characterized as either conservative or dissipative, contingent upon the trace of Matrix (7), which is parameterized by b , as given by

$$tr = \frac{\partial \dot{x}_1}{\partial x_1} + \frac{\partial \dot{x}_2}{\partial x_2} + \frac{\partial \dot{x}_3}{\partial x_3} + \frac{\partial \dot{x}_4}{\partial x_4} + \frac{\partial \dot{x}_5}{\partial x_5} = -1 + b \quad (9)$$

System (2) manifests as a dissipative system for $b < 1$, conservative for $b = 1$, and unbounded if $b > 1$. Crucial roles in dictating the system's stability are played by parameters b and c , as illuminated by Theorem 1.

Theorem 1. Stability of System (2) can be adjudicated by parameters b and c , given that p is set to 1, as follows:

- System (2) achieves stability if $b \in (-\infty, 0)$ and $c \in (-0.26376, 0)$.
- System (2) is unstable and non-hyperbolic for $b = 0$.
- System (2) is unstable and unbounded for $b \in (0, 1)$.

The proof was derived by solving the characteristic Eq. (8) to attain the following equation:

$$(b - \lambda) (\lambda^4 + \underbrace{(1)}_A \lambda^3 + \underbrace{(3+c)}_B \lambda^2 + \underbrace{(2-2c)}_C \lambda - \underbrace{2c}_D) = 0 \quad (10)$$

fourth order system

where, $A = 1$, $B = 3 + c$, $C = 2 - 2c$, and $D = -2c$.

Based on Routh–Hurwitz criterion for a fourth order system [43], several conditions must be met from Eq. (10) to ensure system stability.

$$\begin{cases} A > 0 \\ D > 0 \\ (AB - C)C - A^2D > 0 \\ AB - C > 0 \end{cases}$$

- $\rightarrow A = 1 > 0$
- $\rightarrow D > 0 \Rightarrow -2c > 0 \Rightarrow c < 0$
- $\rightarrow AB - C > 0 \Rightarrow 3 + c - (2 - 2c) > 0 \Rightarrow c > -\frac{1}{3}$
- $\rightarrow (AB - C)C - A^2D > 0 \Rightarrow (1 + 3c)(2 - 2c) - (-2c) > 0 \Rightarrow 1 + 3c - 3c^2 > 0 \Rightarrow -0.2637 < c < 1.2637 \Rightarrow c \in (-0.2637, 1.2637)$

The intersecting conditions $c < 0$, $c > -1/3$, and $c \in (-0.2637, 1.2637)$ yield the range $c \in (-0.2637, 0)$. Under these conditions, the stability of system (2) is assured given a parameter value of b within the range $(-\infty, 0)$. Notably, an instability is introduced to system (2) when b equals 0, due to the presence of a non-hyperbolic root. Additionally, system (2) presents instability for parameter values within the range $b \in (0, 1)$ as the presence of a positive root results in unbounded instability.

Remark 1. The insertion of $b = -1$ and $p = 1$ into Eq. (8) enables a classification of the attractors for system (2). The characteristic Eq. (8), with a substituted value of $c = -0.1$ within the range of $(-0.2637, 0)$, results in the equation:

$$(-1 - \lambda) (\lambda^4 + \lambda^3 + 2.9\lambda^2 + 2.2\lambda + 0.2) = 0$$

This equation yields the roots: $\lambda_1 = -1$, $\lambda_2 = -0.1050$, $\lambda_3 = -0.7121$, $\lambda_{4,5} = -0.0915 \mp 1.6332i$. The negative nature of the roots λ directs the system's orbits towards the fixed point, thus stabilizing system (2). The roots thereby classify the system as Focus-node, indicative of hidden attractors.

In contrast, the insertion of $c = -0.3$, which falls outside the range $(-0.2637, 0)$, into the characteristic Eq. (8) yields:

$$(-1 - \lambda) (\lambda^4 + \lambda^3 + 2.7\lambda^2 + 2.6\lambda + 0.6) = 0$$

Solving the equation gives the roots: $\lambda_1 = -1$, $\lambda_2 = -0.3423$, $\lambda_3 = -0.6999$, $\lambda_{4,5} = 0.0211 \mp 1.5824i$. Due to the positive real part of the complex roots $\lambda_{4,5}$, the system classifies as Saddle-Focus, leading to the instability of system (2), thus, suggesting a Self-excited system.

In the mathematical field of differential equations and dynamical systems, one encounters various types of equilibrium points, namely saddle-focus, node-focus, and non-hyperbolic points.

- A Saddle-Focus point, a critical juncture, presents a unique characteristic within the linearized system: it contains one eigenvalue with a positive real part and two complex conjugate eigenvalues with a non-zero real part. Geometrically, the trajectories proximal to a saddle-focus point demonstrate a blend of saddle-like and spiral-like behaviour.

- On the other hand, a Node-Focus point emerges as a critical juncture wherein the linearized system possesses two complex conjugate eigenvalues with negative real parts and non-zero imaginary parts. The distinguishing factor here is the trajectory behaviour, which solely exhibits a spiral-like movement without any semblance of saddle-like behaviour.

- Lastly, non-hyperbolic points are critical junctures in the linearized system, bearing at least one eigenvalue with a zero real part. The geometric behaviour observed near non-hyperbolic points tends to be more multifaceted, potentially including phenomena like bifurcations, limit cycles, and various types of attractors.

The significance of these classifications is underscored in the qualitative analysis of dynamical systems. They shed light on the stability and behaviour of solutions in proximity to these critical points. By analysing the linearized system around these junctures, it becomes feasible to infer aspects about the local dynamics and the potential existence of various orbit or trajectory types within the system.

Remark 2. Table 2 elucidates the root types, stability, and attractors of system (2) as determined by Eq. (8) when the parameters $b = -1$ and $p = 1$ are substituted. Depending on the parameter c , the system oscillates between stability and instability.

Table 2. Shows the system (2) stability and attractors

c	Roots	Type points	Stability	Attractors
0.006	$\lambda_1 = -1$	Saddle-Focus	Unstable	Self-excited
	$\lambda_2 = 0.006$			
	$\lambda_3 = -0.7154$			
-0.27	$\lambda_{4,5} = -0.1453 \mp 1.6682i$	Saddle-Focus	Unstable	Self-excited
	$\lambda_1 = -1$			
	$\lambda_2 = -0.3046$			
-0.2637	$\lambda_3 = -0.7027$	Non-hyperbolic	Critical case	Self-excited Or Hidden
	$\lambda_{4,5} = 0.0036 \mp 1.5885i$			
	$\lambda_1 = -1$			
-0.006	$\lambda_2 = -0.2967$	Node- Focus	Stable	Hidden
	$\lambda_3 = -0.7032$			
	$\lambda_{4,5} = \mp 1.5898i$			
-0.006	$\lambda_1 = -1$	Node- Focus	Stable	Hidden
	$\lambda_2 = -0.006$			
	$\lambda_3 = -0.7151$			
	$\lambda_{4,5} = -0.1395 \pm 1.6641i$			

Remark 3. From a differential equation standpoint, critical cases in the stability theory refer to scenarios where all the eigenvalues of the characteristic polynomial exhibit negative real parts, with at least one eigenvalue possessing a real part equal to zero.

3.1 Lyapunov Exponential and Lyapunov Dimension

The rate of divergence or convergence of nearby trajectories in a dynamical system is effectively quantified by the Lyapunov exponent. This metric provides insights into the long-term behaviour and stability of a system. A dynamical system is suggested to be unstable or exhibit chaotic behaviour when the Lyapunov exponent is positive, while a negative exponent indicates convergence towards a stable equilibrium. Conversely, the Lyapunov dimension aids in identifying the fractal dimension of a chaotic system and evaluating its effective dimensionality by analysing the scaling properties of the Lyapunov exponents.

The Lyapunov dimension, with its ability to capture the complexity and intricacy of the system's attractor, offers significant insight into the nature of the system. Higher Lyapunov dimensions typically suggest more complex systems with an increased number of degrees of freedom.

Based on numerical simulations conducted using the Wolf Algorithm [44], Figure 3 represents the Lyapunov exponent's spectrum for typical parameters (3) & IC (4):

$$\begin{cases} LE_1 = 0.3049 \\ LE_2 = 0.1218 \\ LE_3 = 0.0027 \\ LE_4 = -0.0002 \\ LE_5 = -1.1293 \end{cases} \Rightarrow \sum_{i=1}^5 LE_i = -0.7001$$

The sum of the first five exponents is $\sum_{i=1}^5 LE_i = -0.7001$, which is approximately equal to $\text{tr}(J(E_1)) = -0.7$. This implies that system (2) displays dissipative behaviour. System (2) features a greater Maximum Lyapunov Exponent (MLE) ($LE_1 = 0.3049$) compared to system (1) ($LE_1 = 0.163$), highlighting its distinctness and higher efficiency. The presence of two positive Lyapunov exponents in system (2) is indicative of its hyperchaotic nature.

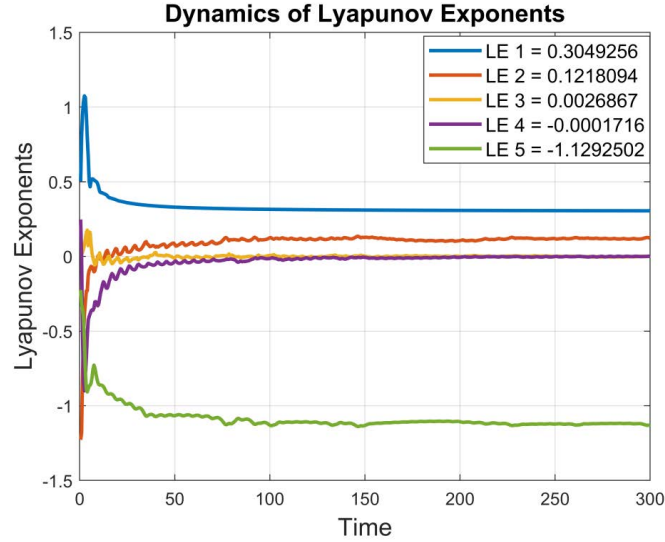


Figure 3. The system's three positive Lyapunov exponents (2) with typical parameters (4), and IC (5)

The Lyapunov dimension of a system is crucial in characterizing the degree of chaotic behaviour. According to the Kaplan-Yorke conjecture [45], the Lyapunov dimension is defined as:

$$D_L = J + \frac{1}{|LE_{J+1}|} \sum_{i=1}^J LE_i \Rightarrow D_L = 4 + \frac{\sum_{i=1}^4 LE_i}{|LE_5|} = 4.3801$$

With taking different values for control parameters and initial condition, in Table 3 and Table 4. Different types of chaotic were obtained.

Table 3. LE_S of the system (2) for a different initial condition with parameters (3)

IC	LE_1	LE_2	LE_3	LE_4	LE_5	Sign of LE_S	Behavior
0.1, 0.1, 0.3, 0.4, 0.5	0.3049	0.0302	0.0011	0.0001	-1.0362	(+, +, +, 0, -)	Hyperchaotic
0.01, 0.2, 0, 0.7, 0.8	0.2994	0.1583	0.0017	-0.0009	-1.1585	(+, +, +, 0, -)	Hyperchaotic
0.3, 0.1, 0.2, 0.1, 0.7	0.3046	0.1274	0.0006	-0.0053	-1.1273	(+, +, 0, -, -)	Hyperchaotic
0.1, 0.1, 0.2, 0.1, 0.4	0.3049	0.0893	0.0001	0.0008	-1.0952	(+, +, 0, 0, -)	Hyperchaotic 2-tours

Table 4. LE_S of the system (2) for different b with parameters (3) and IC (4)

b	LE_1	LE_2	LE_3	LE_4	LE_5	Sign of LE_S	Behavior
0.8	0.7991	0.1401	0.0031	0.0007	-1.1430	(+, +, +, 0, -)	Hyperchaotic
0.02	0.1506	0.0146	-0.0002	-0.0026	-1.1423	(+, +, 0, -, -)	Hyperchaotic
0.94	0.9397	0.1394	0.0001	-0.0005	-1.1387	(+, +, 0, 0, -)	Hyperchaotic 2-tours
0.002	0.1003	-0.0007	-0.0016	-0.0031	-1.0929	(+, 0, -, -, -)	Chaotic
0.0029	0.1101	0.0001	0.0001	-0.0019	-1.1055	(+, 0, 0, -, -)	Chaotic 2-tours

3.2 Multistability

Multistability, a hallmark of complex systems like nonlinear systems or systems with feedback loops, is an underpinning concept across multiple fields, including physics, biology, economics, and engineering. It is essential for elucidating phenomena such as phase transitions, cell differentiation, decision-making processes, and pattern formation. The significance of understanding and analyzing multistability in dynamical systems cannot be understated as it offers deep insights into the behavior of the system, enables accurate predictions of system responses to perturbations, and aids in the design of control strategies aimed at guiding the system towards specific attractors or states.

Evidence of multistability in system (2) is presented in this section, showcasing how various attractors can coexist within the same parameter region, provided the initial conditions are varied. These findings, encapsulated in Table 5, highlight the diverse dynamical behavior the system can display under different initial conditions.

Figure 4 further reinforces these observations, illustrating the coexistence of distinct dynamical behaviors within the new system.

Table 5. Multistability with parameter $a, p = 1$, different b, c and IC

Figure 4	Parameters	Initial Conditions	Color
Figure 4 (a)	$b=0.002$ $c=0.002$	(0.1, 7, 9, 0.2, 0.2)	Red
		(12, 5, 5, 0.5, 0.2)	Blue
		(-12, 6.5, 6, 0.2, 0.9)	Magenta
Figure 4 (b)	$b=0.3$ $c=0.006$	(0.5, 0.3, 2, 2, 0.2)	Red
		(-0.1, 1, 1, 1, 1)	Blue
		(0.1, 0.1, 1, 2, 2)	Magenta
Figure 4 (c)	$b=0.9$ $c=0.004$	(30, 0.1, 0.1, 0.1, 0.1)	Red
		(-30, -0.1, -0.1, -0.1, -0.1)	Blue

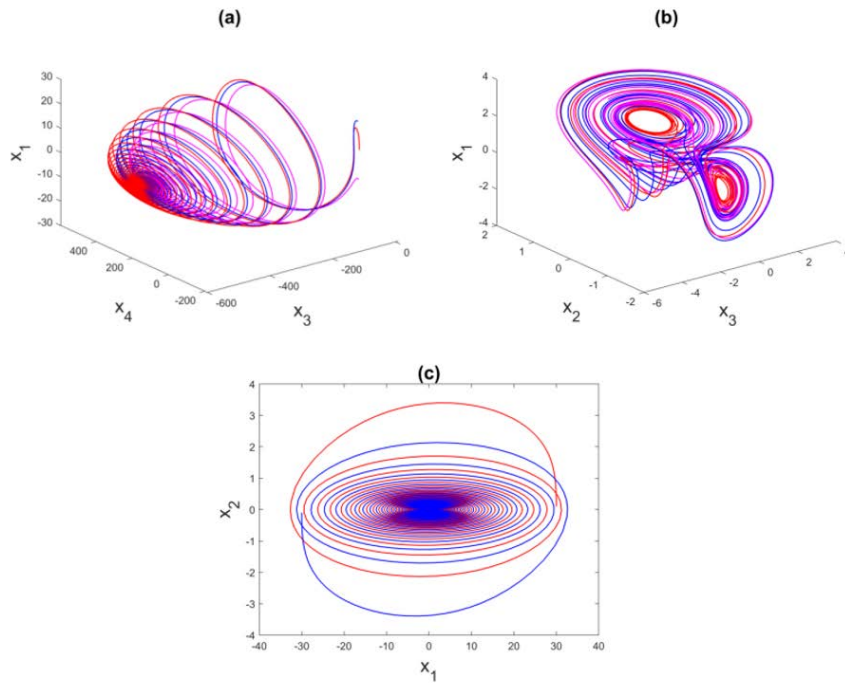


Figure 4. The system's (3) coexistence attractor in (a) $x_3 - x_4 - x_1$ space. (b) $x_3 - x_2 - x_1$ space, (c) $x_1 - x_2$ plane

4 Discussion

Insights gleaned from Table 6 underscore the enhanced efficacy of the newly implemented system (2), particularly when contrasted against the performance of the original system (1).

5 Anti-Synchronization

Projective synchronization bifurcates into two distinctive types: Complete Synchronization (CS) and Anti-Synchronization (AS). The possibility of synchronization was initially doubted until its existence was first observed by Fujisaka and Yamada in 1983 [46]. However, it was not until 1990 when the phenomenon received notable attention, following Pecora and Carrol's discovery of this occurrence between two identically chaotic systems bearing different initial values [47]. This discovery was subsequently christened Complete Synchronization (CS).

The phenomenon known as Anti-Synchronization (AS) is characterized by the asymptotic reduction of the sum of the drive and response systems to zero. In other words, Anti-Synchronization can manifest between a drive system and a response system when the states of the synchronized systems share the same absolute values, yet display opposite signs, implying that all elements of $(\alpha = -1)$ [48]. In this section, a systematic process for the

Table 6. Comparison between the new 5D system and 3D Sprott C system

Details	3D Sprott C System	New 5D system (2)
Equilibria points $E_{1,2}$	$(\pm 1, \pm 1, 0)$	$\left(\pm 1, \pm 1, -\frac{1}{p}, \pm \frac{a}{bp}, \mp \frac{1}{cp}\right)$
Sign of LE_s	$(+, 0, -)$ chaotic	$(+, +, +, 0, -)$ hyperchaotic $(+, +, 0, -, -)$ hyperchaotic $(+, +0, 0, -)$ hyperchaotic 2-torus $(+, 0, -, -, -)$ chaotic $(+, 0, 0, -, -)$ chaotic 2-torus
Type point	• Non-hyperbolic unstable	• \rightarrow Stable focus-nodes • \rightarrow Saddle-focus unstable • \rightarrow Non-hyperbolic unstable
Attractors behavior	Self-excited	Hidden & Self-excited
Max. LE_s	0.163	0.3049
Lyapunov dimension D_L	2.140	4.3801

anti-synchronization of chaos is proposed. The drive systems are represented by system (2), and the corresponding response system is described as follows:

$$\begin{cases} \dot{y}_1 = y_2 y_3 - c y_5 + u_1 \\ \dot{y}_2 = y_1 - y_2 + u_2 \\ \dot{y}_3 = 1 - y_1^2 + u_3 \\ \dot{y}_4 = a y_1 y_3 + b y_4 + u_4 \\ \dot{y}_5 = y_1 + p y_2 y_3 + u_5 \end{cases} \quad (11)$$

The error dynamics in Anti-Synchronization (AS) are defined as: $e_i = y_i - \alpha x_i$, where $i = 1, 2, 3, 4, 5$, $\alpha = -1$, fulfilling the condition:

$$\lim_{t \rightarrow \infty} \|e_i(t)\| = \|y_i - \alpha x_i\| = 0.$$

The error dynamical system is as follows:

$$\begin{cases} \dot{e}_1 = -c e_5 + e_2 e_3 - x_2 e_3 - x_3 (y_2 - x_2) + u_1 \\ \dot{e}_2 = e_1 - e_2 + u_2 \\ \dot{e}_3 = 2 - e_1^2 + 2 x_1 y_1 + u_3 \\ \dot{e}_4 = b e_4 + a e_1 e_3 - a x_1 e_3 - a x_3 (y_1 - x_1) + u_4 \\ \dot{e}_5 = e_1 + p e_2 e_3 - p x_2 e_3 - p x_3 (y_2 - x_2) + u_5 \end{cases} \quad (12)$$

Theorem 2. If designed nonlinear control as follows:

$$\begin{cases} u_1 = -e_1 - e_2 + e_1 e_3 - e_5 - a e_3 e_4 + x_3 (y_2 - x_2) \\ u_2 = -e_1 e_3 - p e_3 e_5 \\ u_3 = -e_3 - 2 + a x_1 e_4 + x_2 e_1 - 2 x_1 y_1 + p x_2 e_5 \\ u_4 = -2 b e_4 + a x_3 (y_1 - x_1) \\ u_5 = c e_1 - e_5 + p x_3 (y_2 - x_2) \end{cases} \quad (13)$$

Then the error dynamical system (12) is asymptotically stable.

Proof. By inserting the proposed controller (13) into Eq. (12), we obtain

$$\begin{cases} \dot{e}_1 = -e_1 - e_2 - (c + 1)e_5 + e_2 e_3 - x_2 e_3 + e_1 e_3 - a e_3 e_4 \\ \dot{e}_2 = e_1 - e_2 - e_1 e_3 - p e_3 e_5 \\ \dot{e}_3 = -e_3 - e_1^2 + a x_1 e_4 + x_2 e_1 + p x_2 e_5 \\ \dot{e}_4 = -b e_4 + a e_1 e_3 - a x_1 e_3 \\ \dot{e}_5 = -e_5 + p e_2 e_3 - p x_2 e_3 + (c + 1)e_1 \end{cases} \quad (14)$$

In accordance with Lyapunov stability theory, we choose a Lyapunov function as follows: $V(e_i) = e^T P e$, $i = 1, 2, \dots, 5$, $P = \text{diag}\{0.5, 0.5, \dots, 0.5\}$, i.e.,

$$V(e_i) = \underbrace{\begin{bmatrix} 0.5 & 0 & 0 & 0 & 0 \\ 0 & 0.5 & 0 & 0 & 0 \\ 0 & 0 & 0.5 & 0 & 0 \\ 0 & 0 & 0 & 0.5 & 0 \\ 0 & 0 & 0 & 0 & 0.5 \end{bmatrix}}_P \begin{bmatrix} e_1 \\ e_2 \\ e_3 \\ e_4 \\ e_5 \end{bmatrix} \quad (15)$$

and their derivative Lyapunov as:

$$\dot{V}(e_i) = e_1 \dot{e}_1 + e_2 \dot{e}_2 + e_3 \dot{e}_3 + e_4 \dot{e}_4 + e_5 \dot{e}_5 \quad (16)$$

$$\begin{aligned} \dot{V}(e_i) = & e_1 [-e_1 - e_2 - (c+1)e_5 + e_2e_3 - x_2e_3 + e_1e_3 - ae_3e_4] \\ & + e_2 [e_1 - e_2 - e_1e_3 - pe_3e_5] + e_3 [-e_3 - e_1^2 + ax_1e_4 + x_2e_1 + px_2e_5] \\ & + e_4 [-be_4 + ae_1e_3 - ax_1e_3] + e_5 [-e_5 + pe_2e_3 - px_2e_3 + (c+1)e_1] \end{aligned} \quad (17)$$

$$\dot{V}(e_i) = -e_1^2 - e_2^2 - e_3^2 - be_4^2 - e_5^2 \Rightarrow \dot{V}(e_i) = - \underbrace{\begin{bmatrix} 1 & 0 & 0 & 0 & 0 \\ 0 & 1 & 0 & 0 & 0 \\ 0 & 0 & 1 & 0 & 0 \\ 0 & 0 & 0 & b & 0 \\ 0 & 0 & 0 & 0 & 1 \end{bmatrix}}_{Q_1} \begin{bmatrix} e_1 \\ e_2 \\ e_3 \\ e_4 \\ e_5 \end{bmatrix}$$

where, $Q_1 = \text{diag}(1, 1, 1, b, 1)$, $b = 0.3$, this yields that $Q_1 > 0$, thus $\dot{V}(e_i)$ is negative definite matrix on R^5 . The corresponds law $\lim_{t \rightarrow \infty} \|e_i(t)\| = 0$ satisfied and the drive and response systems is anti-synchronize. Time series of anti-synchronization for error dynamical system (12) are depicted in Figure 5, with the ICs (0.5, 0.1, -0.2, 0.3, -0.3), and (0.1, -0.2, 0.4, 0.2, 0.1), Figure 6 provides a numerical explanation of the anti-synchronization between (2) and (11), this demonstrates that the theoretical results **Theorem 2**.

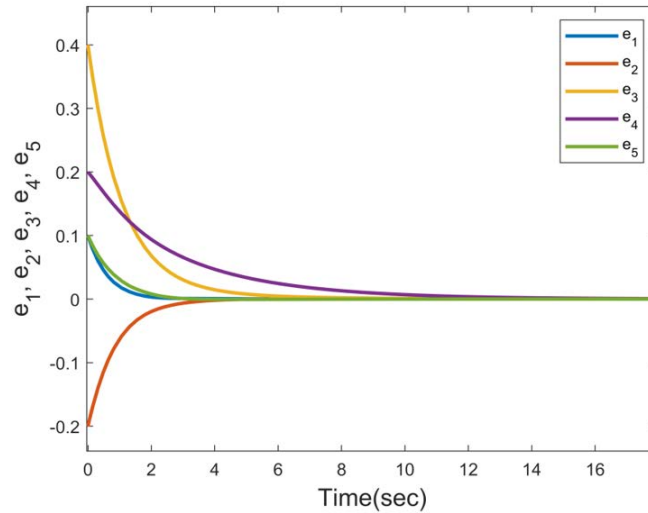


Figure 5. Time series of anti-synchronization for error dynamical system (12) with controller (13)

6 Conclusions

In this study, a novel five-dimensional hyperchaotic system has been introduced, composed of ten terms and evolved from a three-dimensional Sprott C system. This unique system is characterized by the exhibition of two coexisting attractors: a self-excited attractor and a hidden attractor. Various attributes derived from diverse types of

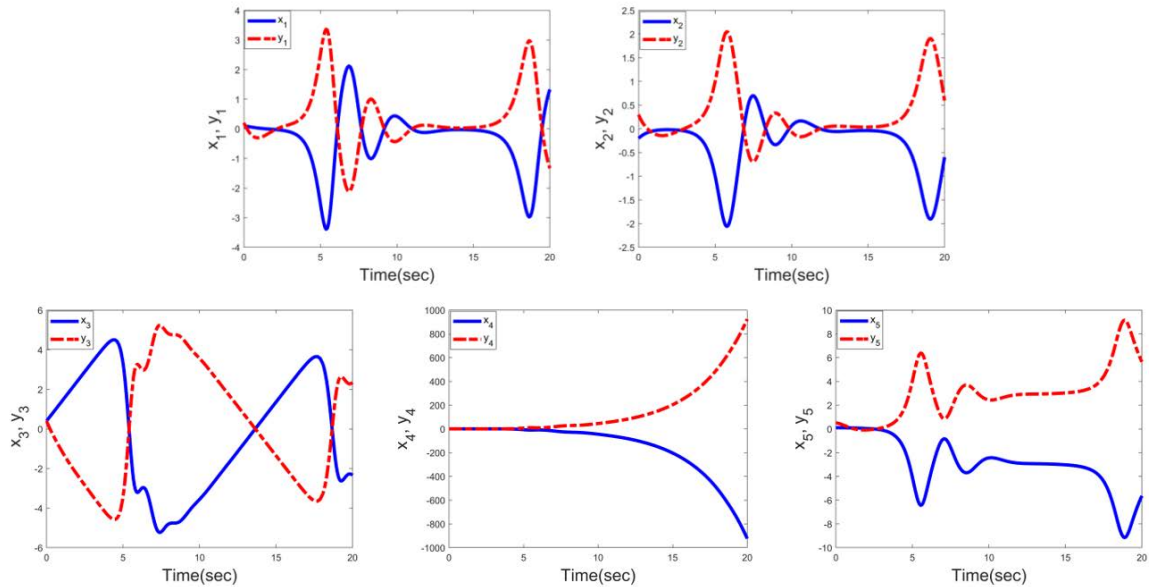


Figure 6. The anti-synchronization (AS) with controller (13)

equilibrium points, such as stable focus-nodes, saddle-focus, and non-hyperbolic unstable points, are incorporated into the system, the presence of which is dictated by the system parameters. The occurrence of chaotic and hyperchaotic attractors coexisting within a single five-dimensional system that accommodates three types of equilibrium points presents a compelling phenomenon.

A plethora of numerical methods, including phase portraits, Lyapunov exponents, Lyapunov dimensions, and Multistability, have been utilized to elucidate the distinct attractors. Furthermore, the synchronization issue of the proposed system is scrutinized extensively in the study by employing stability theory. A myriad of dynamic behaviors, including hyperchaotic, hyperchaotic with 2-tours, chaotic, and chaotic with 2-tours, have been documented. Both theoretical proofs and numerical simulations, executed with MATLAB 2021, have confirmed the legitimacy of these theoretical findings.

This study's impact extends beyond the establishment of the new hyperchaotic system. By unveiling the complexity and richness of the dynamical behaviors within the five-dimensional system, it provides insights for a deeper understanding of chaotic dynamics. Additionally, the identification of different types of equilibrium points under various parameters underscores the role of parameter values in shaping a system's behavior. The coexistence of different types of attractors in the same system also offers a valuable case study of the complex dynamics of hyperchaotic systems. Future research could further explore the implications of these findings for system control and synchronization, potentially opening new avenues for practical applications in secure communication, signal processing, and complex network dynamics.

Data Availability

The data supporting our research results are included within the article or supplementary material.

Conflicts of Interest

The authors declare no conflict of interest.

References

- [1] K. W. Wong, L. Qiuzhen, and C. Jianyong, "Simultaneous arithmetic coding and encryption using chaotic maps," *IEEE Trans. Circuits Syst. II: Exp. Briefs*, vol. 57, no. 2, pp. 146–150, 2010. <https://doi.org/10.1109/TCSII.2010.2040315>
- [2] Z. N. Al-Kateeb and S. J. Mohammed, "Encrypting an audio file based on integer wavelet transform and hand geometry," *Telecommun. Comput. Electron. Control*, vol. 18, no. 4, pp. 2012–2017, 2020. <https://doi.org/10.12928/telkomnika.v18i4.14216>
- [3] S. A. Fadhel, Z. N. Al-Kateeb, and M. J. Al-Shamdeen, "An improved data hiding using pixel value difference method and hyperchaotic system," *J. Phys.: Conf. Ser.*, vol. 1879, no. 2, p. Article ID: 022089, 2021. <https://doi.org/10.1088/1742-6596/1879/2/022089>

- [4] Z. N. Al-Kateeb, M. J. Al-Shamdeen, and F. S. Al-Mukhtar, "Encryption and steganography a secret data using circle shapes in colored images," *J. Phys.: Conf. Ser.*, vol. 1591, no. 1, p. Article ID: 012019, 2020. <https://doi.org/10.1088/1742-6596/1591/1/012019>
- [5] W. Huang and Y. Huang, "Chaos of a new class of hopfield neural networks," *Appl. Math. Comput.*, vol. 206, no. 1, pp. 1–11, 2008. <https://doi.org/10.1016/j.amc.2008.08.041>
- [6] A. S. Al-Obeidi and S. F. Al-Azzawi, "Chaos synchronization of a class 6-d hyperchaotic lorenz system," *Model. Meas. Control B*, vol. 88, no. 1, pp. 17–22, 2019. https://dx.doi.org/10.18280/mmc_b.880103
- [7] C. K. Volos, I. M. Kyprianidis, and I. N. Stouboulos, "Experimental investigation on coverage performance of a chaotic autonomous mobile robots," *Robot. Auton. Syst.*, vol. 61, no. 12, pp. 1314–1322, 2013. <https://doi.org/10.1016/j.robot.2013.08.004>
- [8] A. S. Al-Obeidi and S. F. Al-Azzawi, "A new simple 6d hyperchaotic system with hyperbolic equilibrium and its electronic circuit," *Iraqi J. Comput. Sci. Math.*, vol. 4, no. 1, pp. 155–166, 2023. <https://doi.org/10.52866/ijcsm.2023.01.01.0013>
- [9] G. A. Leonov, N. V. Kuznetsov, and V. I. Vagaitsev, "Localization of hidden chia's attractors," *Phys. Lett. A*, vol. 375, no. 23, pp. 2230–2233, 2011. <http://dx.doi.org/10.1016/j.physleta.2011.04.037>
- [10] E. N. Lorenz, "Deterministic nonperiodic flow," *J. Atmos. Sci.*, vol. 20, no. 2, pp. 130–141, 1963.
- [11] O. E. Rossler, "An equation for continuous chaos," *Phys. Lett. A*, vol. 57, no. 5, pp. 397–398, 1976. [https://doi.org/10.1016/0375-9601\(76\)90101-8](https://doi.org/10.1016/0375-9601(76)90101-8)
- [12] J. C. Sprott, "Some simple chaotic flows," *Phys. Rev. E*, vol. 50, no. 2, pp. R647–R647, 1994. <https://doi.org/10.1103/PhysRevE.50.R647>
- [13] S. T. Kingni, S. Jafari, H. Simo, and P. Wofo, "Three-dimensional chaotic autonomous system with only one stable equilibrium: Analysis, circuit design, parameter estimation, control, synchronization and its fractional-order form," *Eur. Phys. J. Plus*, vol. 129, no. 5, pp. 1–16, 2014. <https://doi.org/10.1140/epjp/i2014-14076-4>
- [14] Q. Deng, C. Wang, and L. Yang, "Four-wing hidden attractors with one stable equilibrium point," *Int. J. Bifurc. Chaos*, vol. 30, no. 6, p. 2050086, 2020. <https://doi.org/10.1142/S0218127420500868>
- [15] Q. Yang, L. Yang, and B. Ou, "Hidden hyperchaotic attractors in a new 5d system based on chaotic system with two stable node-foci," *Int. J. Bifurc. Chaos*, vol. 29, no. 7, p. Article ID: 1950092, 2019. <https://doi.org/10.1142/S0218127419500925>
- [16] A. Ahmadi, K. Rajagopal, F. E. Alsaadi, V. T. Pham, F. E. Alsaadi, and S. Jafari, "A novel 5d chaotic system with extreme multi-stability and a line of equilibrium and its engineering applications: circuit design and FPGA implementation," *Iranian J. Sci. Technol., Trans. Electr. Eng.*, vol. 44, no. 1, pp. 59–67, 2020. <https://doi.org/10.1007/s40998-019-00223-5>
- [17] J. P. Singh and B. K. Roy, "Coexistence of asymmetric hidden chaotic attractors in a new simple 4-d chaotic system with curve of equilibria," *Optik*, vol. 145, pp. 209–217, 2017. <https://doi.org/10.1016/j.ijleo.2017.07.042>
- [18] J. Bao and Y. Liu, "Multistability and bifurcations in a 5d segmented disc dynamo with a curve of equilibria," *Adv. Differ. Equ.*, vol. 2019, no. 1, p. Article ID: 345, 2019. <https://doi.org/10.1186/s13662-019-2284-0>
- [19] L. Gong, R. Wu, and N. Zhou, "A new 4d chaotic system with coexisting hidden chaotic attractors," *Int. J. Bifurc. Chaos*, vol. 30, no. 10, p. Article ID: 2050142, 2020. <https://doi.org/10.1142/S0218127420501424>
- [20] O. S. Ojoniyi and A. N. Njah, "A 5d hyperchaotic sprott b system with coexisting hidden attractors," *Chaos, Solitons & Fractals*, vol. 87, pp. 172–181, 2016. <https://doi.org/10.1016/j.chaos.2016.04.004>
- [21] Z. Wei, I. Moroz, J. C. Sprott, A. Akgul, and W. Zhang, "Hidden hyperchaos and electronic circuit application in a 5d self-exciting homopolar disc dynamo," *Chaos: An Interdiscip. J. Nonlinear Sci.*, vol. 27, no. 3, p. Article ID: 033101, 2017. <https://doi.org/10.1063/1.4977417>
- [22] J. P. Singh and B. K. Roy, "Multistability and hidden chaotic attractors in a new simple 4-d chaotic system with chaotic 2-torus behaviour," *Int. J. Dynam. Control*, vol. 6, pp. 529–538, 2018. <https://doi.org/10.1007/s40435-017-0332-8>
- [23] S. Zhang, X. Wang, and Z. Zeng, "A simple no-equilibrium chaotic system with only one signum function for generating multidirectional variable hidden attractors and its hardware implementation," *Chaos*, vol. 30, no. 5, p. Article ID: 053129, 2020. <https://doi.org/10.1063/5.0008875>
- [24] S. Zhang and Y. Zeng, "A simple jerk-like system without equilibrium: Asymmetric coexisting hidden attractors, bursting oscillation and double full feigenbaum remerging trees," *Chaos. Solit. Fract.*, vol. 120, pp. 25–40, 2019. <https://doi.org/10.1016/j.chaos.2018.12.036>
- [25] Q. Yang and C. Chen, "A 5d hyperchaotic system with three positive lyapunov exponents coined," *Int. J. Bifurc. Chaos*, vol. 23, no. 6, p. Article ID: 1350109, 2013. <https://doi.org/10.1142/S0218127413501095>
- [26] S. Dadras, H. R. Momeni, G. Qi, and Z. Wang, "Four-wing hyperchaotic attractor generated from a new 4d system with one equilibrium and its fractional-order form," *Nonlinear Dyn.*, vol. 67, no. 2, pp. 1161–1173,

2012. <https://doi.org/10.1007/s11071-011-0060-0>

- [27] H. Yu, G. Cai, and Y. Li, "Dynamic analysis and control of a new hyperchaotic finance system," *Nonlinear Dyn.*, vol. 67, no. 3, pp. 2171–2182, 2012. <https://doi.org/10.1007/s11071-011-0137-9>
- [28] S. F. Al-Azzawi and A. S. Al-Obeidi, "Chaos synchronization in a new 6d hyperchaotic system with self-excited attractors and seventeen terms," *Asian-Eur. J. Math.*, vol. 14, no. 05, p. 2150085, 2021. <https://doi.org/10.1142/S1793557121500856>
- [29] S. Y. Al-hayali and S. F. Al-Azzawi, "An optimal nonlinear control for anti-synchronization of rabinovich hyperchaotic system," *Indonesian J. Electr. Eng. Comput. Sci.*, vol. 19, no. 1, pp. 379–386, 2020. <http://doi.org/10.11591/ijeecs.v19.i1.pp380-387>
- [30] M. A. Al-Hayali and F. S. Al-Azzawi, "A 4d hyperchaotic sprott s system with multistability and hidden attractors," *J. Phys.: Conf. Ser.*, vol. 1879, no. 3, p. 032031, 2021. <https://doi.org/10.1088/1742-6596/1879/3/032031>
- [31] S. F. Al-Azzawi and M. A. Al-Hayali, "Coexisting of self-excited and hidden attractors in a new 4d hyperchaotic sprott-s system with a single equilibrium point," *Arch. Cont. Sci.*, vol. 32, no. 1, pp. 37–56, 2022. <https://doi.org/10.24425/acs.2022.140863>
- [32] R. Wang, M. Li, Z. Gao, and H. Sun, "A new memristor-based 5d chaotic system and circuit implementation," *Complexity*, vol. 2018, p. Article ID: 6069401, 2018. <https://doi.org/10.1155/2018/6069401>
- [33] S. Vaidyanathan, V. T. Pham, and C. K. Volos, "A 5-D hyperchaotic rikitake dynamo system with hidden attractors," *Eur. Phys. J. Spec. Top.*, vol. 224, no. 8, pp. 1575–1592, 2015. <https://doi.org/10.1140/epjst/e2015-02481-0>
- [34] J. P. Singh, K. Rajagopal, and B. K. Roy, "A new 5D hyperchaotic system with stable equilibrium point, transient chaotic behaviour and its fractional-order form," *Pramana - J Phys*, vol. 91, no. 3, pp. 1–9, 2018. <https://doi.org/10.1007/s12043-018-1599-9>
- [35] S. Vaidyanathan, L. G. Dolvis, K. Jacques, C. H. Lien, and A. Sambas, "A new five-dimensional four-wing hyperchaotic system with hidden attractor, its electronic circuit realisation and synchronisation via integral sliding mode control," *Int. J. Model. Identific. Con.*, vol. 32, no. 1, pp. 30–45, 2019. <https://doi.org/10.1504/IJMIC.2019.101959>
- [36] G. Hu, "Generating hyperchaotic attractors with three positive lyapunov exponents via state feedback control," *Int. J. Bifurc. Chaos*, vol. 19, no. 2, pp. 651–660, 2009. <https://doi.org/10.1142/S0218127409023275>
- [37] N. T. Nguyen, T. Q. Bui, G. Gagnon, P. Giard, and G. Kaddoum, "Designing a pseudo-random bit generator with a novel 5D-hyperchaotic system," *arXiv preprint arXiv:2105.08896*, 2021.
- [38] S. F. Al-Azzawi and M. A. Al-Hayali, "Multistability and hidden attractors in a novel simple 5D chaotic sprotte system without equilibrium points," *J. Interdiscip. Math.*, vol. 25, no. 5, pp. 1279–1294, 2022. <https://doi.org/10.1080/09720502.2021.1970948>
- [39] K. Benkouider, S. Vaidyanathan, A. Sambas, E. Tlelo-Cuautle, A. A. Abd El-Latif, B. Abd-El-Atty, and P. Kumam, "A new 5-D multistable hyperchaotic system with three positive lyapunov exponents: Bifurcation analysis, circuit design, fpga realization and image encryption," *IEEE Access*, vol. 10, pp. 90 111–90 132, 2020. <https://doi.org/10.1109/ACCESS.2022.3197790>
- [40] B. Fan and L. R. Tang, "A new five-dimensional hyperchaotic system and its application in ds-cdma," in *2012 9th International Conference on Fuzzy Systems and Knowledge Discovery, Chongqing, China, 29-31 May 2012*, 2012, pp. 2069–2073. <https://doi.org/10.1109/FSKD.2012.6233786>
- [41] L. Liu, C. Du, X. Zhang, J. Li, and S. Shi, "Dynamics and entropy analysis for a new 4-D hyperchaotic system with coexisting hidden attractors," *Entropy*, vol. 21, no. 3, p. 287, 2019. <https://doi.org/10.3390/e21030287>
- [42] Q. Yang and M. Bai, "A new 5D hyperchaotic system based on modified generalized lorenz system," *Nonlinear Dyn.*, vol. 88, no. 1, pp. 189–221, 2017. <https://doi.org/10.1007/s11071-016-3238-7>
- [43] S. F. Al-Azzawi, "Stability and bifurcation of pan chaotic system by using routh–hurwitz and gardan methods," *Appl. Math. Comput.*, vol. 219, no. 3, pp. 1144–1152, 2012. <https://doi.org/10.1016/j.amc.2012.07.022>
- [44] A. Wolf, J. B. Swift, H. L. Swinney, and J. A. Vastano, "Determining lyapunov exponents from a time series," *Physica D: Nonlinear Phenom.*, vol. 16, no. 3, pp. 285–317, 1985. [https://doi.org/10.1016/0167-2789\(85\)90011-9](https://doi.org/10.1016/0167-2789(85)90011-9)
- [45] P. P. Singh and B. K. Roy, "Memristor-based novel complex-valued chaotic system and its projective synchronisation using nonlinear active control technique," *Eur. Phys. J. Spec. Top.*, vol. 228, no. 10, pp. 2197–2214, 2019. <https://doi.org/10.1140/epjst/e2019-900036-5>
- [46] T. Yamada and H. Fujisaka, "Stability theory of synchronized motion in coupled oscillator systems. ii: The mapping approach," *Prog. Theor. Phys.*, vol. 69, no. 1, pp. 32–47, 1983. <https://doi.org/10.1143/PTP.69.32>
- [47] L. M. Pecora and T. L. Carroll, "Synchronization in chaotic systems," *Phys. Rev. Lett.*, vol. 64, no. 8, pp.

821–825, 1990. <https://doi.org/10.1103/PhysRevLett.64.821>

- [48] J. Hu, S. Chen, and L. Chen, “Adaptive control for anti-synchronization of chua’s chaotic system,” *Phys. Lett. A*, vol. 339, no. 6, pp. 455–460, 2005. <https://doi.org/10.1016/j.physleta.2005.04.002>